GEOPHYSICS, VOL. 72, NO. 5 (SEPTEMBER-OCTOBER 2007); P. B121–B132, 13 FIGS., 2 TABLES.
10.1190/1.2754667

Case History

3D baseline seismics at Ketzin, Germany: The CO_2SINK project

Christopher Juhlin[1], Rüdiger Giese[2], Kim Zinck-Jørgensen[3], Calin Cosma[4], Hesam Kazemeini[1], Niklas Juhojuntti[1], Stefan Lüth[2], Ben Norden[2], and Andrea Förster[2]

ABSTRACT

A 3D 25-fold seismic survey with a bin size of 12 by 12 m and about 12 km^2 of subsurface coverage was acquired in 2005 near a former natural gas storage site west of Berlin, as part of the five-year EU funded CO_2SINK project. Main objectives of the seismic survey were to verify earlier geologic interpretations of structure based on vintage 2D seismic and borehole data and to map, if possible, the reservoir pathways in which the CO_2 will be injected at 650 m depth, as well as providing a baseline for future seismic surveys and planning of drilling operations. The uppermost 1000 m are well imaged and show an anticlinal structure with an east-west striking central graben on its top that extendsdown to the target horizon. About 30 m of throw is seen on the bounding faults. No faults are imaged near the planned drill sites. Remnant gas, cushion and residual gas, is present near the top of the anticline in the depth interval of about 250–400 m and has a clear seismic signature; both higher amplitudes in the reservoir horizons and velocity pulldown are observed. Amplitude mapping of these remnant gas horizons shows that they do not extend as far south as the injection site, which is located on the southern flank of the anticline. Amplitude anomalies, gas chimneys along an east-west striking fault, show that the stored or remnant gas either has been or is presently migrating out of the reservoir formations. Summed amplitude mapping of the planned injection horizon indicates that this lithologically heterogeneous formation may be more porous at the injection site.

INTRODUCTION

Storage of CO_2 in saline aquifers is, perhaps, the most promising and relevant sequestration option for Europe. Saline aquifers are ubiquitous, and their storage capacity exceeds that of depleted oil and gas fields. The CO_2SINK project (Förster et al., 2006), officially started in April 2004, is aimed at developing an in situ laboratory for CO_2 storage to fill the gap between numerous conceptual engineering and scientific studies on geological storage and a full-fledged onshore sequestration demonstration. Major objectives of the project are to (1) advance the understanding of the science and practical processes involved in underground storage of CO_2 to reduce emissions of greenhouse gases to the atmosphere, (2) build confidence towards future European CO_2 geologic storage, and (3) provide operational field experience to aid in the development of harmonized regulatory frameworks and standards for CO_2 geologic storage.

The in situ laboratory selected for the project is the Ketzin anticline near Berlin, Germany (Figure 1). The site includes industrial land and some infrastructure, which makes it suitable as a testing ground for a small-scale demonstration of CO_2 injection. Natural gas (methane) was stored at the site at depths of 250–400 m in Jurassic sandstones until the year 2000. The site was abandoned in 2004, but infrastructure from the facility is still partially in place. These sandstones, together with interlayered mudstone, siltstone, and anhydrite form a shallow multiaquifer system. The target formation for injec-

Manuscript received by the Editor December 15, 2006; revised manuscript received March 8, 2007; published online August 2, 2007.
[1]Uppsala University, Department of Earth Sciences, Uppsala, Sweden. E-mail: christopher.juhlin@geo.uu.se; hesam.kazemeini@geo.uu.se; niklas.juhojuntti@geo.uu.se.
[2]GeoForschungsZentrum Potsdam, Potsdam, Germany. E-mail: rudi@gfz-potsdam.de; slueth@gfz-potsdam.de; norden@gfz-potsdam.de; for@gfz-potsdam.de.
[3]GEUS, Copenhagen, Denmark. E-mail: kzj@geus.dk.
[4]Vibrometric Oy, Vantaa, Finland. E-mail: calin.cosma@vibrometric.com.

tion of CO_2 lies deeper, at depths of 500–700 m, in the lithologically heterogeneous Upper Triassic Stuttgart Formation. Plans are to drill three boreholes, one injection borehole and two observation boreholes with a spacing of about 50–100 m, into the flank of the Ketzin anticline down to the Stuttgart Formation. Nearly pure CO_2 will be injected into the saline-water-bearing sandstone units at a rate of approximately 100 tons/day for a period of up to two years, starting in late 2007.

An important component of the project is monitoring the movement of injected CO_2 using seismic methods. Seismic monitoring methods that will be applied include crosswell, vertical seismic profile (VSP), moving source profiling (MSP), and 2D and 3D time lapse techniques. In 2004, surface seismic sources were tested in a pilot study at the Ketzin site (S. Yordkayhun et al., personal communication, 2007) for the 3D baseline seismic survey that was acquired in 2005. Main objectives of the 3D survey were to (1) provide, if possible, an understanding of the structural geometry for flow pathways within the reservoir, (2) provide a baseline for later evaluation of the time evolution of rock properties as CO_2 is injected into the reservoir, and (3) provide detailed subsurface images near the injection borehole for planning the drilling operations. The baseline seismic survey contained two components: a full 3D survey of the entire area using a weight-drop source, and a focused pseudo-3D survey near the injection site using a VIBSIST source (Park et al., 1996; Cosma and Enescu, 2001). The latter seismic survey will be repeated within the project framework to add a surface time lapse component to the study.

In this paper, we focus on presenting results from the 3D baseline seismic survey that covers an area of about 12 km^2 (subsurface coverage). We first present background information on the geologic setting, acquisition, and processing before summarizing our interpretations. We find that the geologic structure of the anticline is well imaged to target depth and below. Both important seismic horizons and subvertical faults near the top of the anticline can be mapped. In addition, the seismic data allow us to map the extent of remnant storage gas that was not removed from the aquifers when the site was abandoned in 2004. Finally, we comment on the field parameters used in the survey and our potential capability to track movements of the injected CO_2 at this site with seismic methods.

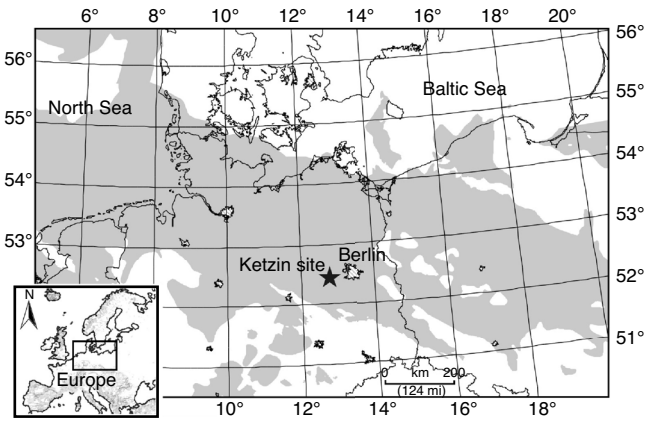

Figure 1. Location of the Ketzin site in the mid-European Permian Basin (gray shaded). Map after Lokhorst (1998). Figure from Förster et al. (2006).

GEOLOGIC SETTING

The Ketzin site (Figure 1) is located in the Northeast German Basin (NEGB), part of a Permian basin system that extends from the southern North Sea across Denmark, The Netherlands and northern Germany to Poland (Ziegler, 1990). The development of the basin system began with initial rifting in the early Permian. Subsidence followed the rifting with the deposition of Permian clastic rocks and the Upper Permian Zechstein salt. A phase of accelerated subsidence, which started in the late Permian, was followed by relatively low subsidence rates from the middle Triassic to early Jurassic. Major rift- and wrench-tectonics in the Triassic, Jurassic, and early Cretaceous in western and central Europe, entailing a renewed destabilization of the lithosphere, only affected the North German platform to a minor degree (Ziegler et al., 1995). In the NEGB, this renewed tectonic activity resulted only in the formation of local north-northeast–south-southwest directed depocenters (e.g., the Rheinsberg Trough), but no large-scale increased (thermal) subsidence (Scheck and Bayer, 1999). The late Cretaceous and Paleocene compressional/transpressional intraplate deformation in the Alpine foreland of Europe (Ziegler et al., 1995) also affected the NEGB, but also only to a minor degree compared to areas further to the west (e.g., the Lower Saxony Basin) and to the east (the Polish Trough), both of which inverted at that time. The NEGB remained mainly metastable with only some local highs and marginal troughs developing. Since the Triassic, salt flow has formed pillows, walls, and diapirs, resulting in the deformation of the Mesozoic overburden into a system of anticlines and synclines (Kossow et al., 2000). It is on the eastern part of a double anticline, the Roskow-Ketzin anticline, that the Ketzin site is located.

The anticline formed above an elongated salt pillow situated at a depth of 1500–2000 m. The axis of the anticline strikes north-northeast–south-southwest and its flanks dip gently at about 15° (Förster et al., 2006). Triassic (Buntsandstein, Muschelkalk, and Keuper) and Lower Jurassic formations constitute the immediate, structurally deformed overburden above the salt pillow (Figure 2). The stratigraphic succession indicates a first gentle uplift of the Ketzin anticline beginning in the early Triassic. Major uplift began first about 140 Ma ago, resulting in total erosion of the Lower Jurassic/Toarcian and the Middle and Upper Jurassic formations. A second uplift event occurred at 106 Ma that resulted in erosion of Lower Cretaceous rocks. The total thickness of the eroded rocks is on the order of 500 m. Upper Cretaceous rocks were probably never deposited in the area since a structural high existed during these times (Stackebrandt and Lippstreu, 2002). Sediments of the Oligocene (Rupelton) form the first geologic formation unaffected by anticlinal uplift and rest above Jurassic sediments. These transgressive sediments are the first indications of regional downwarping of the central parts of the Northeast German Basin, a process that is still active today (Stackebrandt and Lippstreu, 2002).

The topography of the Ketzin area is relatively flat, but does contain some isolated highs consisting mainly of Quaternary sands. Vintage reflection seismic profiles (Figure 3) and stratigraphic and lithological information from the many shallow boreholes drilled in the area provide information on the local subsurface geology. The target for the CO_2 injection at Ketzin is the 80 m thick and lithologically heterogeneous Stuttgart Formation of Middle Keuper (Upper Triassic) age at depths of 500–700 m (Figure 2). Sandy channel-facies rocks of good reservoir properties alternate with muddy flood-plain-facies rocks of poor reservoir quality within the Stuttgart Formation.

Sandstone intervals may attain a thickness of several tens of meters where subchannels are stacked on top of one another with widths up to several hundreds of meters (Wurster, 1964). Playa-type rocks (of the Weser and Arnstadt formations), consisting mainly of claystone, silty claystone, and anhydrite, form an approximately 210-m-thick caprock section above the Stuttgart Formation. The 10–20 m-thick anhydrite layer is known as the Heldburg-Gips and marks the top of the Weser Formation (Figure 2). This anhydrite layer is mapped as a clear reflection on the vintage regional seismic surveys in the area and has been named the K2 (Keuper) reflector. The top of the anhydrite lies about 80 m above the top of the Stuttgart Formation.

Jurassic sandstones are found above the Arnstadt Formation, between 250 and 400 m depth, and were used for the industrial storage of natural gas until the year 2000. These sandstones, together with interlayered mudstone, siltstone, and anhydrite, form a multiaquifer system. A Tertiary clay (the Rupelton), about 80–90 m thick, forms the caprock for this aquifer system. This Tertiary clay acts as a major aquitard separating the saline waters (brines) in the deeper aquifers from the nonsaline groundwater in shallow Quaternary aquifers. There is evidence that local erosion of the Rupelton aquitard at some locations (Förster et al., 2006) allows saline waters to ascend and mix with the fresh water in the shallow aquifers.

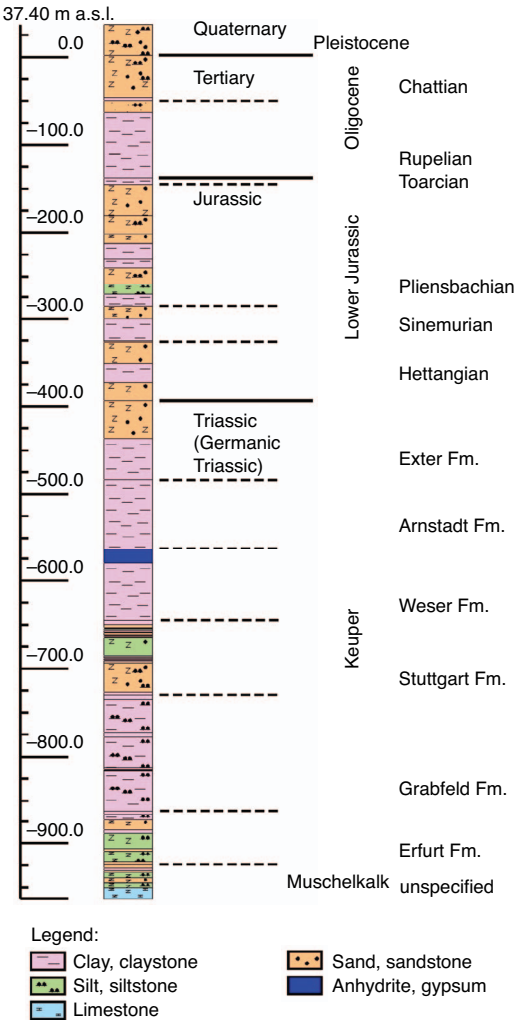

Figure 2. Stratigraphy of the Ketzin area based on drilling of the Ktzi 169/63 borehole. See Figure 3 for location of the borehole.

DATA ACQUISITION

Acquisition was carried out using a template scheme (Table 1), with the aim of having the same acquisition geometry for each template. The template geometry (Figure 3) was a modified version of that used by ETH Zurich in their 3D high-resolution seismic surveys (Spitzer et al., 2001). After all sources had been activated within a template, the receiver locations were then shifted by half a template when moving within a swath. Upon completion of a swath, all active receivers were moved to the next swath and acquisition continued with half of the source locations being the same as in the adjoining template in the previous swath. This overlap of source points and recording stations from template to template gives an even nominal fold of 25 for the survey area. In practice, it was not possible because of logistics such as roads, villages, nature reserves and infrastructure, to have a regular geometry for the templates resulting in the actual fold being less than 25 for some parts of the survey area (Figure 4).

Acquisition began on September 1, 2005 in template 9:5 (Figure 3) and proceeded in a snaking manner through the survey area, finishing on November 20 in template 1:1. No data were acquired in swath 10 and in templates 1:4 and 1.5. About 7500 source points were recorded during the 72 days of active acquisition. In general, each source point consisted of eight hits with the weight drop source. Aside from days that it was necessary to jump swaths, it was possible to activate about 130 source points per day. Line problems and prob-

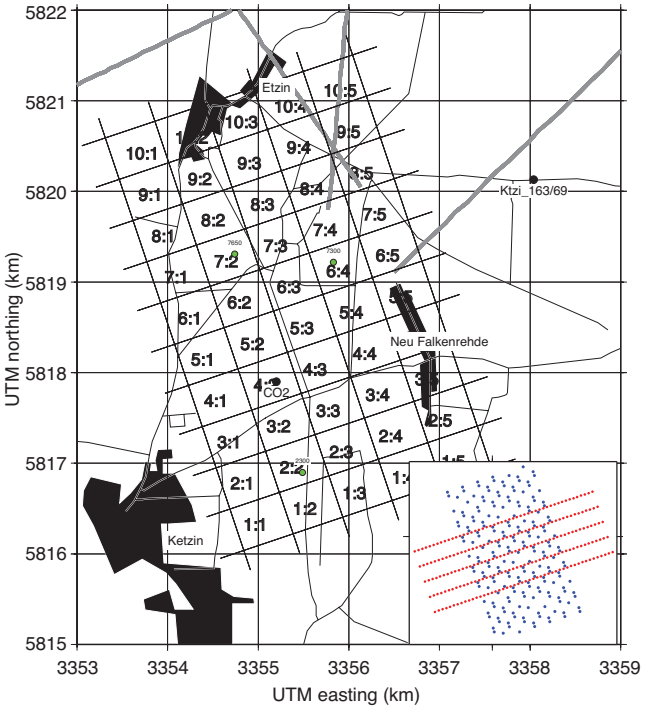

Figure 3. Template system used in the data acquisition, location of the Ktzi 163/69 deep borehole and the planned CO_2 injection site (CO_2). Inset shows theoretical source (blue) and receiver (red) locations for a single template. Green dots show the locations of the three source gathers shown in Figures 5 and 6. Vintage seismic lines in the area are marked by thick gray lines.

lems with the source were generally solved within an hour or less, the only major delays being due to harvesting of crops and construction work at the injection site.

Initially, it was planned that the staking and surveying team should lie three to four templates ahead of the recording team. However, permitting and crop harvest schedules resulted in this gap generally being reduced to one template, implying any delay in staking and surveying would result in a delay in seismic data acquisition. Therefore, lists of points with theoretical coordinates for sources and receivers within each template were delivered to the recording crew by the surveying team one or two days in advance of starting acquisition in the template. Source locations that could not be used due to nature reserves or other obstacles were not included in the lists. The field positions of sources and receivers were located within 1 m of the listed theoretical point coordinates, otherwise a shift was noted in the log. True field coordinates of the marked point were then measured to an accuracy of 0.2 m. In this way, the true coordinates, with only a few exceptions, of all source and receiver points were stored in the raw SEGD files that were recorded onto disks.

Table 1. Template acquisition parameters for the full 3D survey at Ketzin, 2005.

Parameter	Value
Receiver line spacing/number	96 m/5
Receiver station spacing/channels	24 m/48
Source line spacing/number	48 m/12
Source point spacing	24 m or 72 m
CDP bin size	12 m × 12 m
Nominal fold	25
Geophones	28 Hz single
Sampling rate	1 ms
Record length	3 s
Source	240 kg accelerated weight drop, 8–9 hits per source point
Instrument	SERCEL 408UL

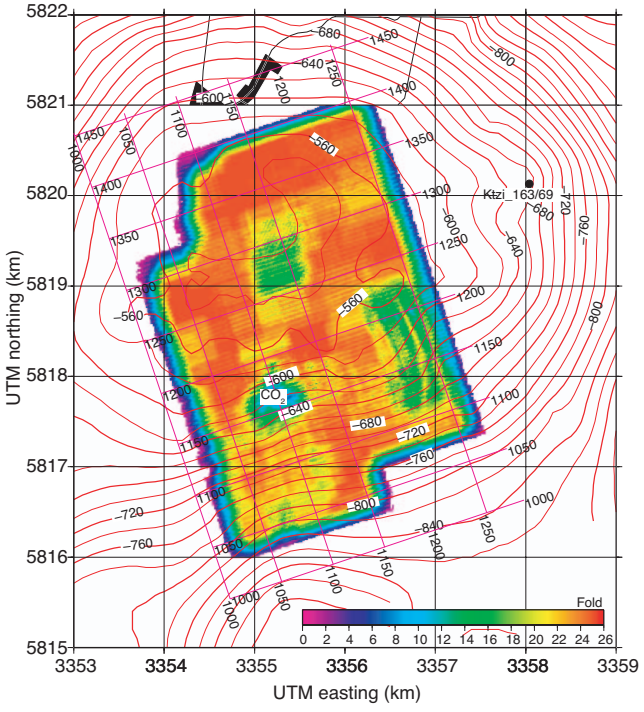

Figure 4. Actual fold for the 3D survey. Shown also are the system of inlines and crosslines for the 3D processing. Isolines indicate the elevation of the estimated top of the Stuttgart Formation based on vintage seismic data and shallow borehole data.

DATA PROCESSING

Processing steps were kept relatively simple (Table 2) to allow the processing to be carried out quickly and to minimize the potential for introducing artifacts into the processed volumes. In-field stacking of the eight or nine weight drop hits consisted of a straight vertical

Table 2. Processing steps applied to the full 3D data set.

Step	Parameters
1	Read raw SEGD data
2	Vertical diversity stack
3	Bulk static shift to compensate for source delay: 6 ms
4	Extract and apply geometry
5	Trace edit and polarity reversal
6	Pick first breaks: offset range 300–500 m
7	Remove 50-Hz noise on selected receiver locations
8	Spherical divergence correction: v^2t
9	Band-pass filter: Butterworth 7–14–150–250 Hz
10	Surface consistent deconvolution: filter 120 ms, gap 16 ms, white noise 0.1%
11	Ground roll mute
12	Spectral equalization 20–40–90–120 Hz
13	Band-pass filter: 0–300 ms: 15–30–85–125 Hz 350–570 ms: 14–28–80–120 Hz 620–1000 ms: 12–25–70–105 Hz
14	Zero-phase filter
15	Refraction statics: datum 30 m, replacement velocity 1800 m/s, v_0 1000 m/s
16	Trace balance using data window
17	Velocity analysis: every 20th CDP in the inline and crossline direction
18	Residual statics
19	Normal moveout correction: 50% stretch mute
20	Stack
21	Trace balance: 0–1000 ms
22	FX-Decon: Inline and crossline directions
23	Trace balance: 0–1000 ms
24	Migration: 3D FD using smoothed stacking velocities
25	Depth conversion: using smoothed stacking velocities

stack. A comparison of the straight vertical stacking with diversity stacking showed that the latter produces superior shot gathers, with higher signal-to-noise ratios. Therefore, the first processing step was to restack the weight drop hits using a diversity stacking method. The timing delay in the weight drop source was reported to be 6.3 ms by the source crew. Field tests confirmed this delay and a 6-ms time shift was applied to all data to shift the data to zero time. A 6-ms time shift was used rather than the measured 6.3-ms shift to avoid interpolation of data values right from the start of the processing.

Geometry was extracted from the SEGD headers and the data were binned into 12×12 m CDP bins. A grid of inlines and crosslines were set up for the processing (Figure 4). The grid was made larger than the actual survey area to ensure the inclusion of all source and receiver points in the present full 3D survey and possible extensions of it. The injection site falls approximately on crossline 1100 and inline 1175. Fold is generally close to 25, but there exist some areas where fold is low because of (1) the gas works at the injection site, (2) nature preserves, and (3) the village of Neu Falkenrehde (Figure 4). Inspection of fold for different offset ranges shows that these three areas have reduced fold for nearly all offset ranges. These plots also show that an acquisition footprint in these areas is likely because of the uneven distribution of longer offsets.

Statics, both refraction and residual, and velocity analysis had the greatest influence on the processed stack. Refraction statics were calculated using a two-layer model with first breaks picked in the 300–500-m offset window. Several tests were done with varying the velocities of the layers, but best results were obtained using an upper layer velocity of 1000 m/s and a lower half space velocity of 1800 m/s, a velocity consistently observed over the entire area for the deeper refractor. The refraction statics due to the model mimicked the topography, while the residual refraction statics were highly variable. Model refraction statics were up to 40 ms on topographic highs, while residual refraction statics were generally on the order of a few ms. Application of the refraction statics nearly always resulted in improved coherency in source and receiver gathers. Two passes of velocity analysis were carried out, one before residual reflection statics and one after. The final velocity field was visually inspected to ensure that there were no sharp jumps in it. Deconvolution and filter panel tests were carried out to determine the optimum parameters for these steps. After a preliminary stack was generated, a filter (step 13) to convert the near minimum-phase wavelet of the weight drop source to a wavelet being closer to zero phase was designed. Several locations in the stacked volume were selected and an average zero-phasing filter was produced. This filter was then applied to the prestack data in order to improve the accuracy of the velocity analysis. No automatic gain control has been applied to the data. However, traces were balanced, prior to velocity analysis and stacking, using the cone of expected P-wave reflections. Trace balancing was applied again after stacking and after FX-deconvolution. For 3D migration, a 30° finite difference code was applied using a smoothed version of the stacking velocity field. The same smoothed stacking velocity field was used for the depth conversion. Although depth converted volumes are available, we have chosen to stay in the time domain for our interpretations. This is because we have little velocity control, resulting from a lack of deeper boreholes in the area.

To illustrate the effects of some of the processing steps on the data, three source points have been selected (Figure 3). Source point 2300 is from an area in the south where the data quality is generally high, source point 7300 contains receivers that were expected to be problematic because they were placed on a topographic high consisting of dry sand close to an active sand and gravel pit, and source point 7650 is from an area where the stacked images appear to be of somewhat poorer quality, possibly resulting from faulting. Statics were also problematic in this area. Ground roll is pronounced on all raw source gathers and masks any reflections that arrive within the noise cone (Figure 5). At source point 7650, power line 50-Hz noise is also pronounced, but could be removed by filtering. Several tests using various multichannel filters to remove the ground roll were made, but with limited success. Therefore, after surface consistent deconvolution, the ground roll was muted (Figure 6). This ground roll tail mute was not applied all the way to zero time in order not to further reduce the fold in the shallowest part of the volume. This may have resulted in some ground roll be stacked into the final volume at some locations. Given that the NMO velocity field varies rather slowly over the area, the 50% stretch mute effectively removed the first breaks and served as a top mute. Application of residual reflection statics further improved the coherency of reflections. In general, the processing steps applied improved the resolution and coherency of the source gathers. However, at locations where the raw gathers are poor, such as source point 7300, the final processed gathers are still of lower quality than at other locations.

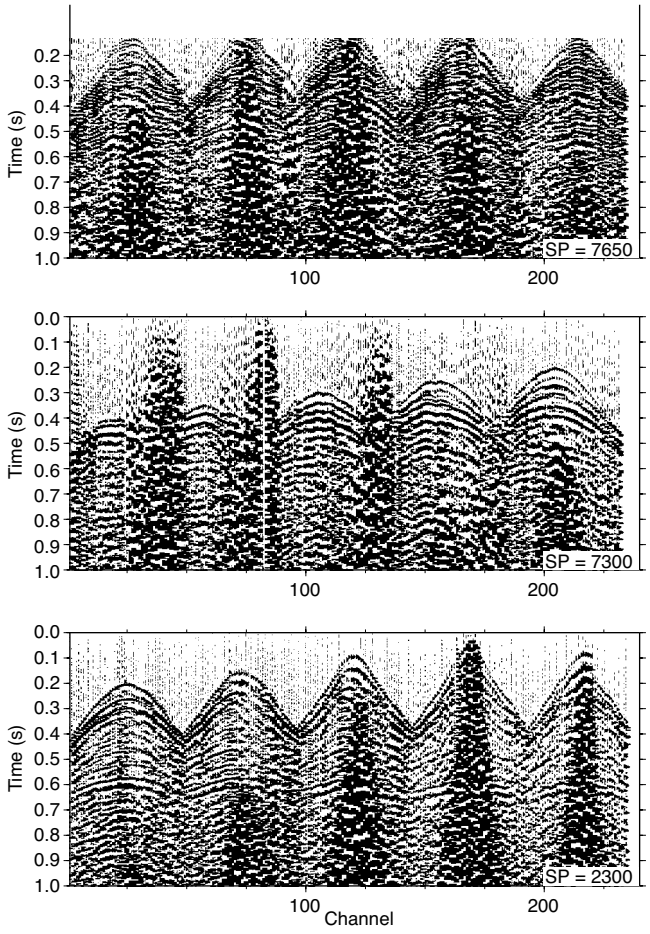

Figure 5. Example of three raw source gathers. Locations of gathers shown in Figure 3.

INTERPRETATION

The subsurface is generally well imaged from about 100 ms down to about 900 ms (Figure 7). Poorer images of the near-surface structure are obtained only where the fold is low (Figure 4). Based on information from borehole data, correlation with seismic data from other parts of the NEGB, and the seismic images themselves, the following reflection horizons were mapped from the migrated volume: (1) near Base Tertiary, (2) near Top Sinemurian, (3) near Top Triassic, (4) near Top Arnstadt Formation, (5) Top Weser Formation, (6) near Top Stuttgart Formation, and (7) near Base Stuttgart Formation (Figure 7). Reflection horizons that could be mapped over the entire area have been run through edge detection algorithms in order to help detect faults. The near Base Tertiary and Top Weser horizons are very well defined because of their characteristic seismic response, and the two horizons can be confidently mapped over the whole area. They are generally present throughout the North German Basin and are known as the T1 (reflection from the transgression phase of the Cenozoic: soft-hard rock boundary) and the K2 (Top Weser Formation), respectively (Reinhardt, 1993). Although less well constrained in the present data set, the reflection horizons corresponding to the near Top Triassic and the near Base Stuttgart Formation are also known on a regional scale as the K1 (reflection from the base of the Exter Formation: sandstone-mudstone boundary) and the K3 (reflection from the top of the Grabfeld Formation: reflection from an anhydrite layer). Below, we give a brief overview of the main structural features of the seismic data.

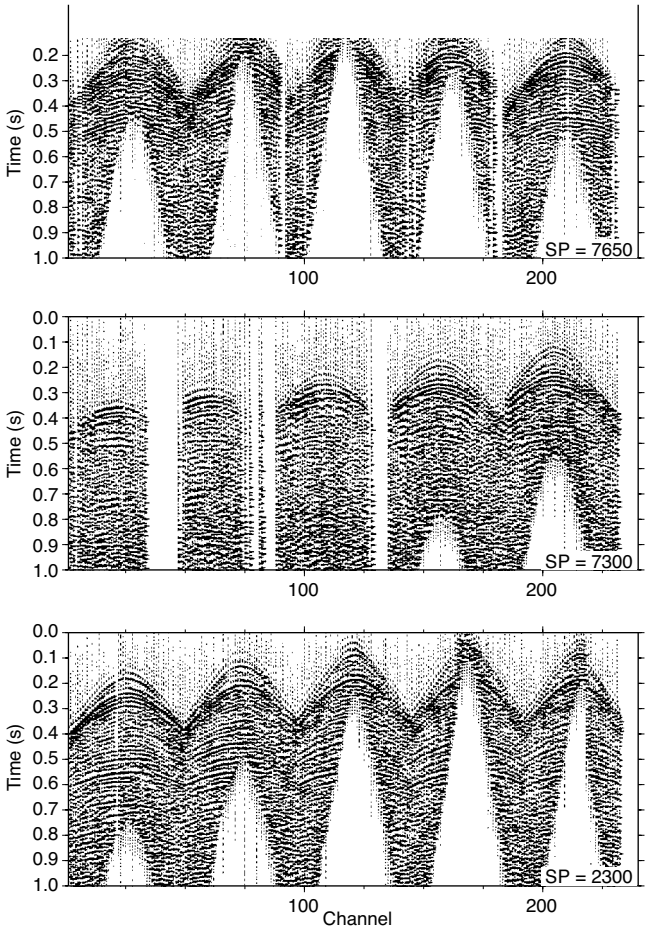

Figure 6. Source gathers from Figure 5 with processing applied up to step 16 in Table 2. Locations of gathers shown in Figure 3.

General structure

The internal structure of the Quaternary and Tertiary layers in the surveyed area is not resolved by the present processing of the 3D seismic data. The strong reflection from near the Base Tertiary unconformity, at approximately 150–180 ms (Figure 7), is the first clear seismic event that can be identified with certainty. It consists of a strong double reflection (trough-peak-trough), and the near Base Tertiary has been picked in the uppermost trough. The underlying parallel, dome-shaped layers are truncated by the subhorizontal near Base Tertiary reflection.

The near Base Tertiary time structure map and edge detection map (Figure 8) reveal several interesting structures. The subhorizontal to slightly dome-shaped horizon is intersected by several curved lineaments. In the northern part of the area a number of east-west– to west-southeast–east-northeast–trending lineaments define an approximately 600–800 m wide depressed area referred to as the Central Graben Fault Zone (CGFZ). On seismic sections (Figure 7), it is clearly seen that the lineaments represent an east-west–trending fault zone across the central part of the Ketzin structure.

South of the CGFZ, two subparallel, curved ridges trend from east to west, apparently following the contours of the sub-Tertiary structural dome. The ridges are not seen in the seismic sections below or above and are believed to represent a subcrop pattern, i.e., erosional features in the Top Jurassic paleotopography (questa-like ridges forming in relative competent lithologies).

Two small circular structures in the Base Tertiary maps (one at the planned CO_2 injection site and one in the central part of the graben area), as well as two small, north-northwest–trending features in the eastern part of the area, do not represent geologic structures, but are the result of the acquisition geometry (lower fold areas in Figure 4).

Sandstones of Upper Sinemurian age comprise the uppermost reservoir in which natural gas was stored until the year 2000. Remnant gas is clearly identified on the 3D seismic data near the Top Sinemurian reflection horizon by velocity pull-down and amplitude

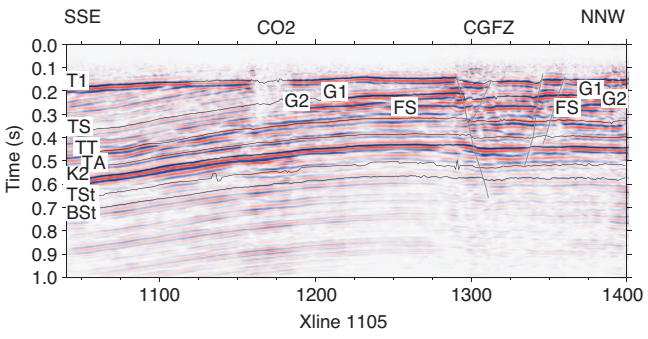

Figure 7. Crossline 1105 crossing nearly over the top of Ketzin anticline. Mapped reflection horizons are (1) near Base Tertiary (T1), (2) near Top Sinemurian (TS), (3) near Top Triassic (TT), (4) near Top Arnstadt Formation (TA), (5) Top Weser Formation (K2), (6) near Top Stuttgart Formation (TSt), and (7) near Base Stuttgart Formation (BSt). CGFZ, G1, G2, and FS indicate the upper gas layer, the lower gas layer, and the flat spot, respectively. Depth in kilometers corresponds roughly to time in seconds since rms velocities vary from about 1700 to 2400 m/s down to the target depth.

brightening (Figure 7). Thus, the horizon is fairly well constrained in the crestal part of the Ketzin anticline. In the area clearly affected by the presence of remnant stored gas, the Top Sinemurian is assumed to be represented by the uppermost reflection (a trough). The Top Sinemurian defines a dome-shaped structure. In the crestal area, the reflection is located less than 100 ms below the Base Tertiary, whereas towards the southern flank, it is located approximately 200 ms below the Base Tertiary.

The near-Top Triassic horizon is fairly well defined and has been picked in a relatively strong peak, approximately 100 ms below the Top Sinemurian (Figure 7). In contrast, the near Top Arnstadt Formation does not appear to be represented by a particular seismic event. It has been picked in a peak approximately 70 ms below the near Top Triassic horizon.

The Top Weser Formation is well defined in the seismic data and is characterized by a strong double reflection (trough-peak-trough, Figure 7). The strong reflectivity from this horizon is attributed to a 20-m-thick anhydrite layer in the uppermost part of the formation. As for the Top Sinemurian to Top Arnstadt horizons, the Top Weser horizon forms a gentle structural dome (Figure 9). The east-west–trending CGFZ, described from the Base Tertiary time structure map and edge detection map, is still clearly recognizable at this deeper level.

In the absence of a well-tie, neither the top nor the base (K3) of the Stuttgart Formation can be correlated to any particular seismic event. The top of the formation has been picked, with some uncertainty, in a weak peak approximately 80–90 ms below the Top Weser, and the base of the approximately 80-m-thick formation has been picked in a weak trough about 70 ms later (Figure 7). The CGFZ, or at least its main bounding faults, is also recognizable at the Stuttgart level.

Fault mapping

The 2D vintage seismic data that were acquired in the 1960s across the Ketzin and Roskow structures do not resolve any faults on the Ketzin anticline. This is probably because of the lower frequency content (generally 20–50 Hz), and the sparser source and receiver spacing (160 and 80 m, respectively) of these lines, as well as their geographic location. However, east-west–trending faults were mapped on the neighboring Roskow anticline, and on the Ketzin anticline a west-southwest–east-northeast– to east-west–trending fault zone was inferred based on well and production data from the former natural gas storage facility. The new 3D seismic data confirm the presence of this latter fault zone (the CGFZ) and, to a large degree, also its location and outline. The west-southwest–east-northeast– to east-west–trending CGFZ is controlled by a series of discrete normal faults, mostly striking west-southwest–east-northeast and east-west. The faults are very well developed in the Jurassic section (Figure 8), but seem to die out quickly in the Rupelian clays (10–50 ms above the base of the Tertiary). The main bounding faults have throws of up to 30 ms (about 30 m) in the Jurassic section. These main faults are also clearly recognizable at the Top Weser level (Figure 9) where the same magnitude of throw is observed (20 ms corresponds to about 30 m at these depths) and, in spite of low overall reflection continuity around the target reservoir, they can occasionally be traced down to and below the Stuttgart Formation. The discrete normal faults of the CGFZ were most likely formed in response to extensional faulting across the crestal part of the Ketzin structure during the main episodes of domal growth (140 and 106 Ma). However, the fault pattern itself suggests that the fault system was not formed in a pure extensional tectonic regime. The northeast– to east-northeast–striking faults that intersect and/or offset the main east-west–striking faults indicate a strike-slip component in the faulting.

The southern part of the CGFZ is located more than 1.5 km north of the planned CO_2 injection site, and no faults at the seismic scale are seen in the vicinity of the injection site. The observation of a

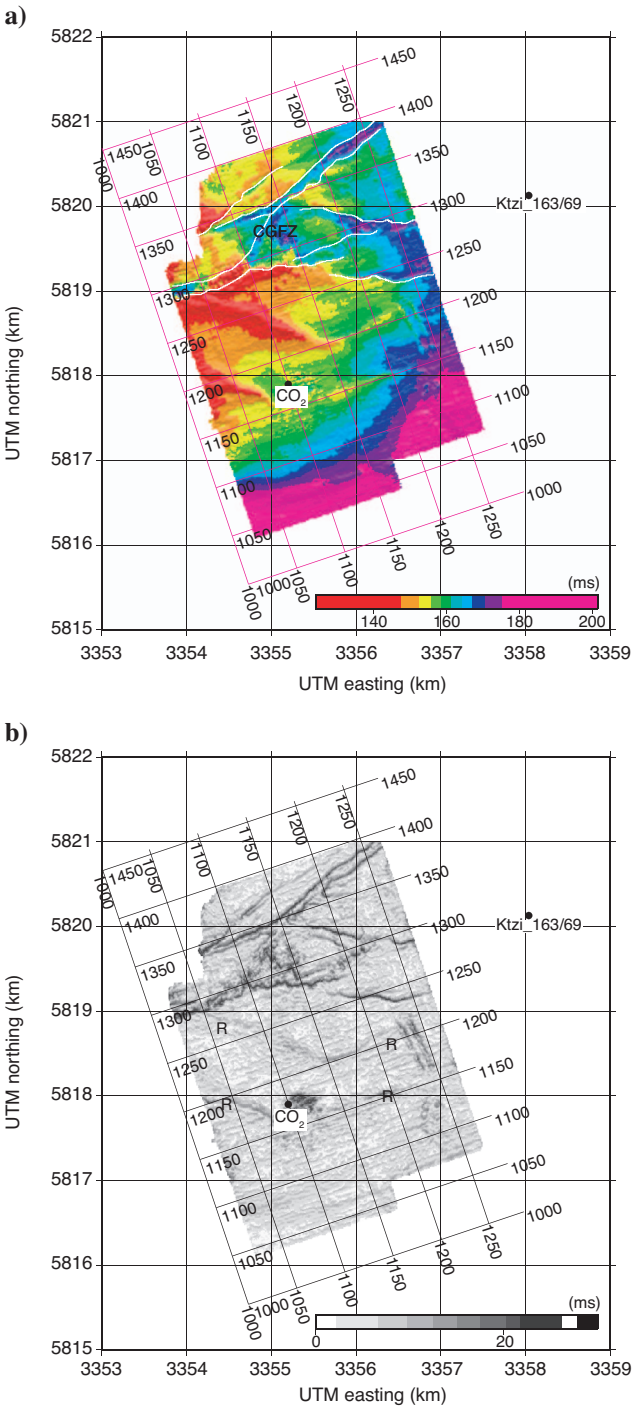

Figure 8. (a) Time horizon map of the T1 (near Base Tertiary) reflection and (b) corresponding edge detection map of the horizon. White lines in (a) mark mapped faults. CGFZ — Central graben fault zone. R — Questa ridges discussed in text.

number of faint, south-east– to south-southeast–striking lineaments on the Top Weser edge detection map (Figure 9) may indicate the presence of small scale faults (1–2 ms of throw corresponds to 1.5–3.0 m) radiating out from the crestal area of the Ketzin dome. Some of these possible faults can be followed up to the Base Tertiary. None of the lineaments, however, intersect the planned injection site, although a few of them are located only a few hundreds of meters away to the south (Figure 9). The closest is seen about 250 m south of the planned injection site.

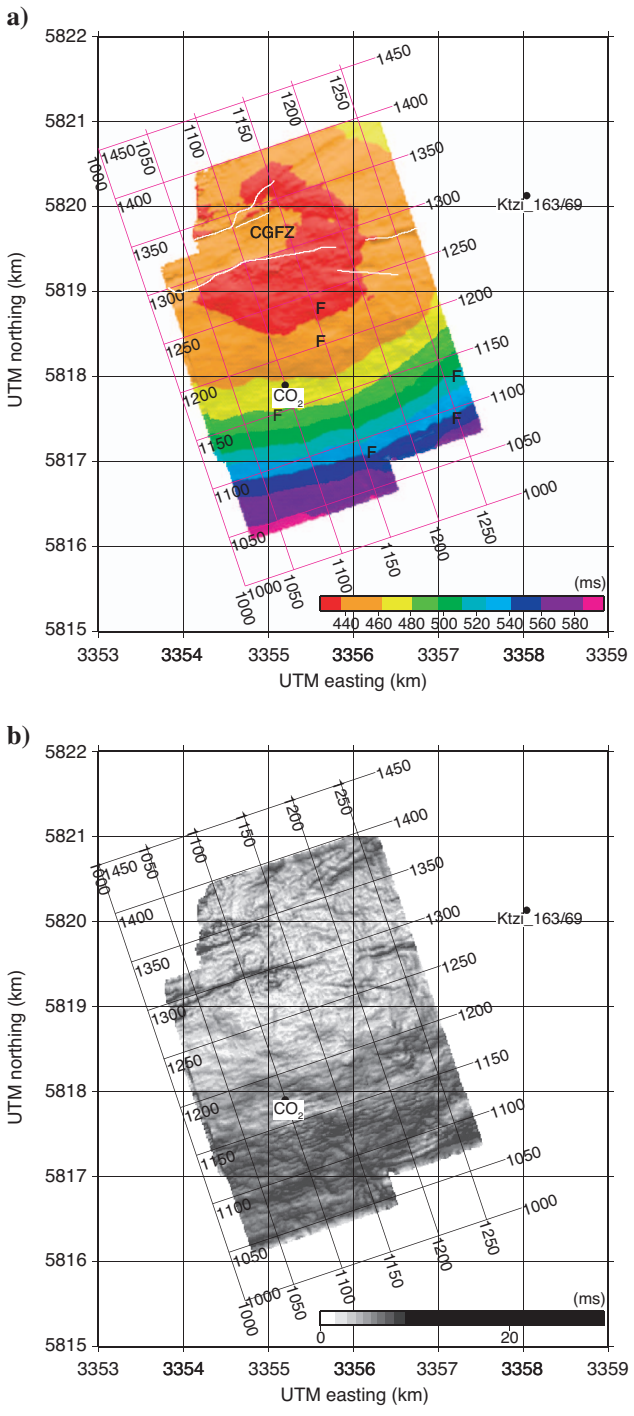

Figure 9. (a) Time horizon map of the K2 (Top Weser Formation) reflection and (b) corresponding edge detection map of the horizon. White lines in (a) mark mapped faults. CGFZ — Central graben fault zone. F — Possible fault with a few ms of throw.

Mapping of remnant stored gas

The Lower Jurassic formations of the Ketzin structure were used for storage of first town gas, and later of natural gas from the 1970s until 2000. According to the operator (UGS Mittenwalde), the maximum utilization of the facility was in 1999. In 2004, the site was abandoned and the reservoir pressure was lowered to approximately 17 bar (UGS, 2005, personal communication) below hydrostatic pressure. Based on information provided by UGS, it is expected that only cushion and residual gas remain in the reservoirs. It is well known that even a small concentration ($<10\%$) of gas in porous rock significantly reduces the P-wave velocity (e.g., Töskoz et al., 1976). Therefore, an aquifer that contains small concentrations of gas will have a significantly different seismic response than if it contains only water. In particular, seismic reflections are expected to be stronger from a partially gas saturated aquifer. Based on this behavior and that gas should tend to accumulate on the top of the Ketzin dome, it is possible to observe in the 3D seismic volume the extent of the aquifers that contain gas. The degree of cushion and residual gas saturation is unknown, but its presence is clearly seen on the new 3D seismic data (Figure 7). Thus, strong amplitude brightening of some of the reflections below the Base Tertiary horizon in the crestal area is seen together with a velocity pull-down along the boundary between the high and low amplitudes. At least two separate gas-bearing layers can be identified in the seismic data. The upper gas layer (the Top Sinemurian horizon) was discussed earlier. The second gas layer is picked approximately 30 ms below the top layer in a trough (Figure 7). For the upper gas layer there appears to be a trend of decreasing amplitude with depth. Locally, in the crestal area, a horizontal reflection, a flat spot, underlies the higher amplitude reflections and is interpreted to represent the maximum gas-water contact of the former gas storage facility when it was operating (Figure 7).

The upper gas layer is very well defined on the seismic data and it is constrained both by the amplitude anomalies, as well as from the velocity pull-down edge (Figure 10). The gas distribution in this layer as determined from the seismic data is in very good accordance with a wellbore-based gas distribution map from UGS. Mapping of the lower gas layer is more difficult because of tuning effects from the flat spot structure below, interference from the fault zones, and the close proximity of the upper gas layer. The gas distribution of layer 2 as given from the amplitude map (Figure 11) should, therefore, only be used to map the boundary of the residual gas towards the south, east, and northeast. The distribution roughly follows the same trend as for the upper gas layer, but there are local differences. For example, in the area just north of the planned injection site the remnant gas of the lower layer reaches further to the south (about 290 m from the injection site) than the gas of the upper layer (about 430 m from the injection site). Such differences may indicate that the two reservoir layers are two separate hydraulic units with an intercalated seal.

A gas chimney, about 1 km long and 100 m wide, has been observed along the southwestern main fault of the CGFZ, i.e., gas-induced amplitude brightening has been observed in a restricted volume along a fault zone (Figure 12). It is located above the upper gas

layer, but below the Base Tertiary, and is probably caused by gas migrating from the Lower Jurassic formations into the fault zone at some stage during the gas storage operation. It is likely that either the reservoir pressure exceeded the fault reactivation pressure, causing the fault to move and, therefore, leak, or the reservoir pressure exceeded the fault capillary entry pressure. As mentioned earlier, both well data and seismic data show that at least some of the other main faults of the CGFZ are sealing. There are no signs of failure of the Rupelian seal above the gas storage area, and, thus, no indications of gas escaping to the Tertiary and Quaternary sections. However, as already noted, the present processing of the 3D data do not provide a good image at these depths.

Seismic resolution of the Stuttgart Formation depositional architecture

The presence and internal architecture of the Stuttgart Formation reservoir rock near the planned injection site is one of the critical as-

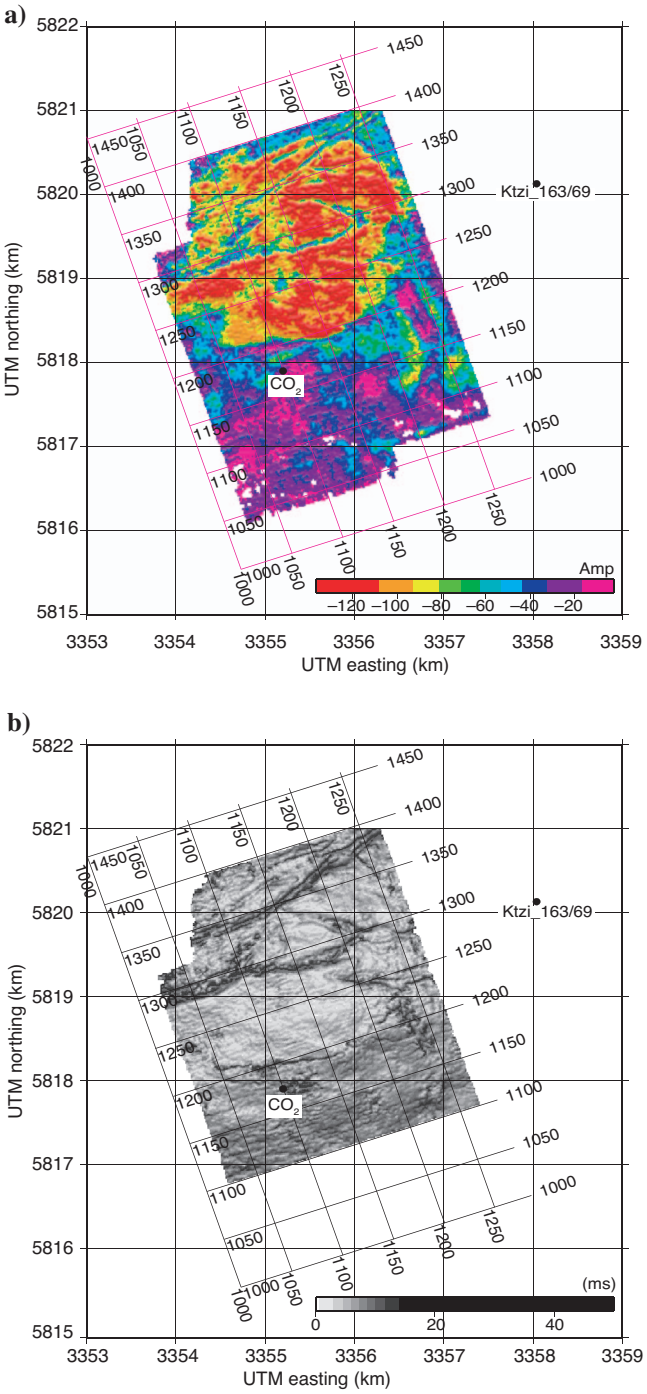

Figure 10. (a) Amplitude map of the Top Sinemurian horizon and (b) edge detection map of the Top Sinemurian horizon.

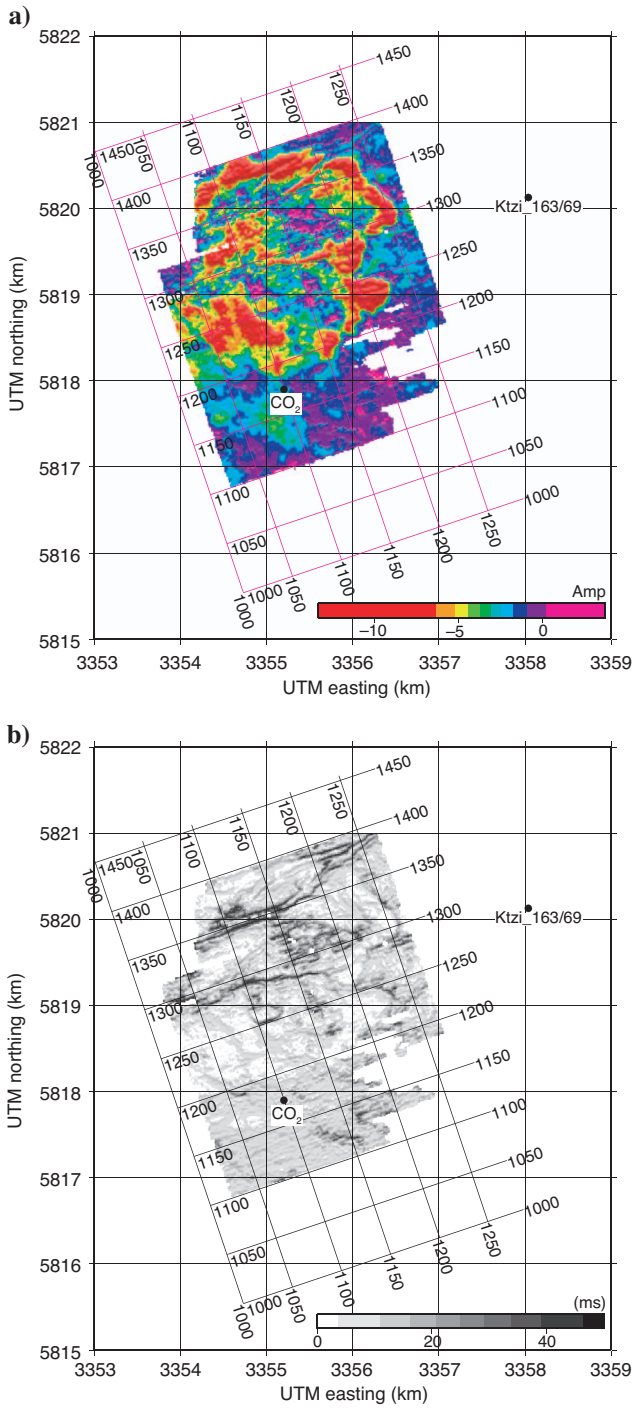

Figure 11. (a) Amplitude map of gas layer 2 and (b) edge detection map of gas layer 2.

pects of the CO_2SINK project. Therefore, it is presently being investigated to determine whether the 3D seismic data can resolve this architecture. Until now, it has not been possible to conclusively map out any internal reservoir architecture. Reservoir bodies are expected to be 100–1000 m wide, by 1–5 km long, by 5–30 m (3–20 ms) high. Smaller reservoir bodies would be below the resolution limit of the seismic data. Although below the resolution, the presence of sand bodies within the Stuttgart Formation may affect the seismic amplitude of reflections from within this unit by increasing them where they are present. A map of the summed amplitude in the time window 20–100 ms below the picked K2 horizon shows the possible distribution of reservoir bodies in the Stuttgart formation as indicated by higher summed amplitude (Figure 13). The general northeast-southwest trend of these amplitude anomalies is consistent with the expected general orientation of the channels. In addition, one of the anomalies appears to project into the Ktzi 163/69 borehole where the Stuttgart Formation was penetrated and is known to contain sandstone (Förster et al., 2006), adding additional support to the interpretation of the higher amplitudes as representing sand channels. If this interpretation is correct, then sand should be expected to be encountered in the Stuttgart Formation at the planned injection site.

DISCUSSION

Time-lapse potential

Time-lapse seismic surveys are an important component of any CO_2 sequestration project (Arts et al., 2004; Sakai, 2004). Within the present project framework, time-lapse crosshole, VSP, MSP, and a repeat of the pseudo-3D star will be carried out. CO_2 will be injected at about 650 m on the southern flank of the Ketzin anticline (Figure 3). Given that the remnant gas of the former gas storage facility is clearly seen on the 3D baseline seismic data, it is therefore expected that the injected CO_2 can be mapped by seismic methods. An important question is what amount of gas is required at depth for it to be detected by these methods. It is expected that the injected CO_2 will migrate towards the top of the Ketzin anticline. Therefore, another important question is to what extent the presence of the remnant gas may mask a seismic response of the injected CO_2 as it migrates. At present, it is not known if the distribution of the remnant gas is static or dynamic.

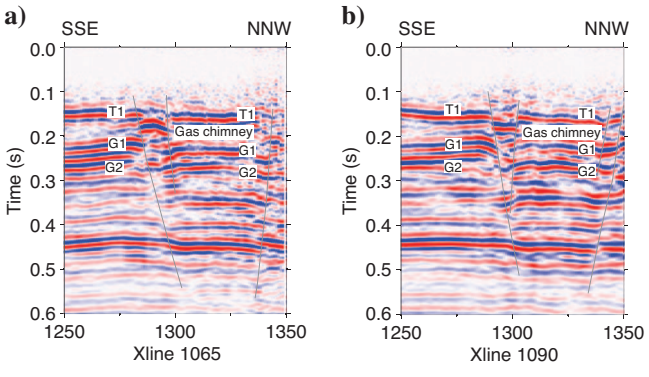

Figure 12. Cross-lines 1065 and 1090 showing the gas chimney. The Base Tertiary (T1) and the upper (G1) and lower (G2) gas layers are also marked. Depth in kilometer corresponds roughly to time in seconds since rms velocities vary from about 1700 to 2400 m/s down to the target depth.

Possible CO_2 migration pathways

The fault zone with the gas chimney can be mapped down to the level of the Stuttgart Formation and is, therefore, a risk factor that must be considered in relation to future CO_2 injection and storage in this formation. The fact that the fault zone was permeable in the Jurassic section at some stage during the natural gas storage operation does not necessarily mean that the fault will be open for CO_2 migration from deeper sections. Likewise, the fact that faults were impermeable for migration of the stored gas does not necessarily mean they will be so for CO_2 migration, given differences in fluid properties. The Stuttgart Formation is at a greater depth than the Jurassic formations and at normal hydrostatic pressure. The rocks have been buried deeper in the past (Förster et al., 2006) and have fairly high yield strengths (Dula, 2006). During operations, the target Stuttgart reservoir will be at lower operating over-pressures than were applied in the Jurassic reservoirs for storage operations. Furthermore, the fault above the Stuttgart Formation intersects the 210 m thick, tight (Springer et al., 2006; Dula, 2006) mudstone and evaporite section. Given these factors, it is unlikely that the fault will be open for fluid flow from the depths of the Stuttgart Formation to shallower levels.

Acquisition and processing considerations

Modern 3D seismic surveys carried out for petroleum exploration purposes generally have thousands of active channels, high fold, use geophone arrays, and require a large number of people in the field. In contrast, data for the Ketzin 3D baseline seismic survey were acquired with only 240 active channels, a fold of 25, single geophones, and a small field crew. Although the environment at Ketzin is similar to that of the Zürcher Weinland survey in Switzerland (Birkhaüser and Graf, 2000), a much smaller acquisition team was used at

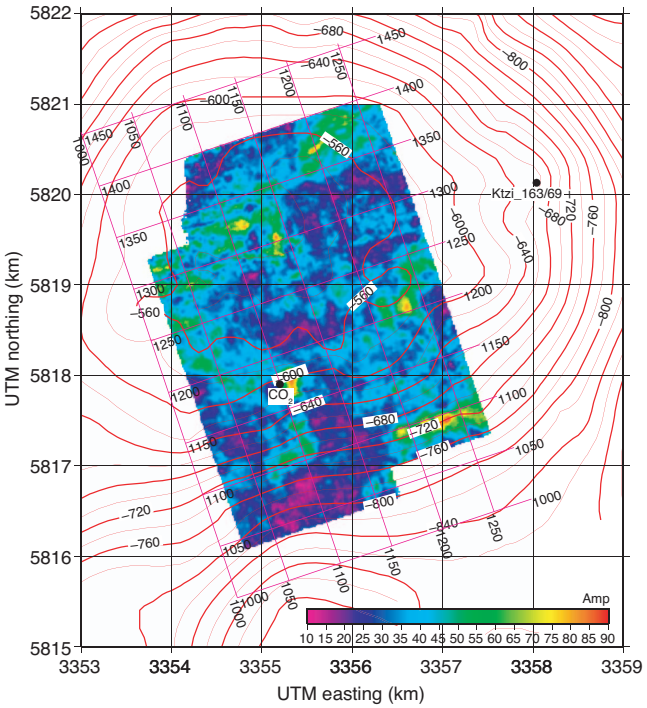

Figure 13. Summed amplitude map for the Stuttgart Formation. Isolines indicate the elevation of the estimated top of the Stuttgart Formation based on vintage seismic data and shallow borehole data.

Ketzin. In spite of this, we have clearly imaged the subsurface down to at least 1000 m. Although a relatively advanced acquisition system was used, it would have been possible to acquire the data with a simpler and cheaper system. If CO_2 sequestration is to be done on a large scale, then it is highly likely that authorities will require both baseline and monitor seismic surveys to be carried out in conjunction with the operation. Our experience shows that it is possible to do this with a relatively small number of channels and people in the field, implying that larger civil and geophysical engineering companies should be able to perform surveys similar to our Ketzin 3D survey. Large scale CO_2 sequestration may open new opportunities for these companies and geophysicists.

Standard processing steps were applied to the data from the Ketzin 3D survey. However, from our experience with the data it is clear that refraction static corrections were probably the most important step in the processing sequence. Experiences from processing data from Canada and Sweden (e.g., Wu and Mereu, 1992; Juhlin, 1995) have also shown the refraction static correction to be, perhaps, the most important step in the processing of high-resolution seismic data. The importance of the refraction static correction implies that it is probably an advantage to use single geophones, rather than arrays, for surveys such as the Ketzin one.

CONCLUSIONS

We acquired 3D seismic data at Ketzin, Germany, with the aim to (1) map the structure of the Ketzin anticline and potential fluid pathways within it, (2) obtain a baseline survey for future time-lapse studies, and (3) provide detailed images near the injection site for planning of drilling operations. Data quality from the full 3D survey is generally good and most of the 3D volume is imaged down to 1 s. In general, the large scale structure is close to that which is expected from shallow drilling and vintage seismic data. No obvious faults are observed near the planned injection site. Clear faults are observed on the top of the Ketzin dome, most of which are oriented in the west-southwest–east-northeast to east-west direction. These faults form a central graben at the top of the anticline and extend down into the formation that CO_2 will be injected into.

Remnant natural gas, cushion and residual gas, from the natural gas storage facility is clearly observed in two aquifers in the form of higher amplitude anomalies in the 200–300 ms window toward the top of the dome. Their geographic extent is similar to that mapped by the gas storage operator (UGS) in 1999 using borehole and pumping data. The remnant gas does not to extend as far south as the planned injection site. Gas has migrated in the past during the operation of the storage facility, or possibly still is migrating, upwards along an approximately 1-km-long stretch of an east-west–striking fault in the northwestern part of the survey area. It is not clear from the seismic data if the gas has/is migrating through the Tertiary Rupelton clay (not imaged on the seismic data) and all the way to the surface. It is also unknown if the remnant gas is in a static state. If not, its presence will make monitoring of injected CO_2 below the top of the anticline more difficult.

A summed absolute amplitude map over the lithologically heterogeneous Stuttgart Formation in a time window encompassing the boundary between the overlying caprock and the target formation shows higher amplitudes near the injection site, indicating possible sandier channels in the formation at this location. The general pattern of the amplitude anomaly is consistent with the expected orientation of channels in the Stuttgart Formation.

Large-scale sequestration of CO_2 is expected to be carried out in the coming decades. It is highly likely that the authorities will require both site and monitor surveys in these operations. Our experience shows that high quality 3D seismic data can be acquired with a small field crew, single geophones, and a simple weight drop source. This observation implies that smaller seismic contractors could be used for siting and monitoring of these future sequestration sites, opening up new opportunities for geophysicists.

ACKNOWLEDGMENTS

We thank several people for input on the seismic acquisition, processing, and interpretation aspects of this work. In particular, we wish to thank the Geophysik-GGD (Leipzig) source crew and the staking and survey crew for good cooperation in the field and Hans Palm for interfacing between the surveying and acquisition teams. We thank R. Lobitz (G.E.O.S. Freiberg) for negotiations with the landowners. We also wish to thank the people from Shell that are involved in the CO_2SINK project. GLOBE Claritas™, under license from the Institute of Geological and Nuclear Sciences Limited, Lower Hutt, New Zealand, was used to process the seismic data. We thank three anonymous reviewers for their constructive criticism. The European Commission is gratefully acknowledged for funding CO_2 Storage by Injection into a Natural Storage site (CO_2SINK), Project no. 502599.

REFERENCES

Arts, R., O. Eiken, A. Chadwick, P. Zweigel, L. van der Meer, and B. Zinszner, 2004, Monitoring of CO_2 injected at Sleipner using time-lapse seismic data: Energy, **29**, 1383–1392.

Birkhaüser, P., and R. Graf, 2000, 3D Seismics in Zürcher Weinland: Methodology, planning and performances of the field work: Nagra Bulletin, 33, 8–17.

Cosma, C., and N. Enescu, 2001, Characterization of fractured rock in the vicinity of tunnels by the swept impact seismic technique: International Journal of Rock Mechanics and Mining Sciences, **38**, 815–821.

Dula, F., 2006, Capillary top seal analysis for CO_2 storage: Implications for Ketzin anticline, Germany: Internal Shell Report EP 2006-5097.

Förster, A., B. Norden, K. Zinck-Jørgensen, P. Frykman, J. Kulenkampff, E. Spangenberg, J. Erzinger, M. Zimmer, J. Kopp, G. Borm, C. Juhlin, C. Cosma, and S. Hurter, 2006, Baseline characterization of the CO_2SINK geological storage site at Ketzin, Germany: Environmental Geosciences, **13**, 145–160.

Lokhorst, A., 1998, NW European gas atlas: Nederlands Institute voor Toegepaste Geowetenschappen TNO, CD-ROM.

Juhlin, C., 1995, Imaging of fracture zones in the Finnsjön area, central Sweden, using the seismic reflection method: Geophysics, **60**, 66–75.

Kossow, D., C. Krawczyk, T. McCann, M. Strecker, and J. F. W. Negendank, 2000, Style and evolution of salt pillows and related structures in the northern part of the Northeast German Basin: International Journal of Earth Sciences, **89**, 652–664.

Park, C. B., R. D. Miller, D. W. Steeples, and R. A. Black, 1996, Swept impact seismic technique (SIST): Geophysics, **61**, 1789–1803.

Reinhardt, H.-G., 1993, Regionales Kartenwerk der Reflexionsseismiok: VEB Geophysik Leipzig.

Sakai, A., 2004, Monitoring of the carbon dioxide sequestration by time-lapse 3D seismic survey in Japan. Paper presented at the 7th International Conference on Greenhouse Gas Control Technologies.

Scheck, M., and U. Bayer, 1999, Evolution of the Northeast German Basin — Inferences from a 3D structural model and subsidence analysis: Tectonophysics, **313**, 145–169.

Spitzer, R., F. O. Nitsche, and A. G. Green, 2001, Minimizing field operations in shallow 3-D seismic reflection surveying: Geophysics, **66**, 1761–1773.

Springer, N., H. Lindgren, and K. Fries, 2006, CO_2SINK: WP 3.1 Rock/fluid interactions, Laboratory experiments. Caprock seal capacity characterisation of old core material from the Ketzin structure: Geological Survey of Denmark and Greenland Report 2006/24.

Stackebrandt, W., and L. Lippstreu, 2002, Zur geologischen Entwicklung Brandenburgs, *in* W. Stackebrandt, and V. Manhenke, Atlas zur Geologie

von Brandenburg im Maßstab 1:1,000,000: Kleinmachnow (Germany), Landesamt für Geowissenschaften und Rohstoffe Brandenburg, 13–18.
Toksöz, M. N., C. H. Cheng, and A. Timur, 1976, Velocities of seismic waves in porous rocks: Geophysics, **41**, 621–645.
Wu, J., and R. F. Mereu, 1992, Crustal structure of the Kapuskasing uplift from Lithoprobe near-vertical/wide angle seismic reflection data: Journal of Geophysical Research, **97**, 17441–17453.
Wurster, P., 1964, Geologie des Schilfsandsteins: Mitt. Geol. Staatsinst. **33**, 140.
Ziegler, P. A., 1990, Geological atlas of western and central Europe: Shell Internationale Petroleum Mij. B. V.
Ziegler, P. A., S. Cloetingh, and J. D. van Wees, 1995, Dynamics of intraplate compressional deformation: The Alpine foreland and other examples: Tectonophysics, **252**, 7–59.